Microfluidic Screening Reveals Heparan Sulfate Enhances Human Mesenchymal Stem Cell Growth by Modulating FGF-2 Transport

Supplementary Information

Drew M. Titmarsh[1], Clarissa L.L. Tan[1], Nick R. Glass[2], Victor Nurcombe[1,3], Justin J. Cooper-White[2,4,5], and Simon M. Cool[1,6*]

[1]Institute of Medical Biology, Agency for Science Technology and Research (A*STAR), 8A Biomedical Grove, #06-06 Immunos, SINGAPORE 138648.

[2]Australian Institute for Bioengineering & Nanotechnology, The University of Queensland, St. Lucia, QLD 4072, AUSTRALIA.

[3]Lee Kong Chian School of Medicine, Nanyang Technological University–Imperial College London, SINGAPORE 308232.

[4]School of Chemical Engineering, The University of Queensland, St. Lucia, QLD 4072, AUSTRALIA.

[5]Biomedical Manufacturing, Manufacturing Flagship, CSIRO, Clayton, Victoria 3169, AUSTRALIA.

[6]Department of Orthopaedic Surgery, Yong Loo Lin School of Medicine, National University of Singapore, SINGAPORE 119074.

*Corresponding author:
Simon Cool, PhD
Institute of Medical Biology
8A Biomedical Grove, #06-06 Immunos, SINGAPORE 138648
Tel +65-64070176 Fax: +65-64789477
Email: simon.cool@imb.a-star.edu.sg

SUPPLEMENTARY FIGURES

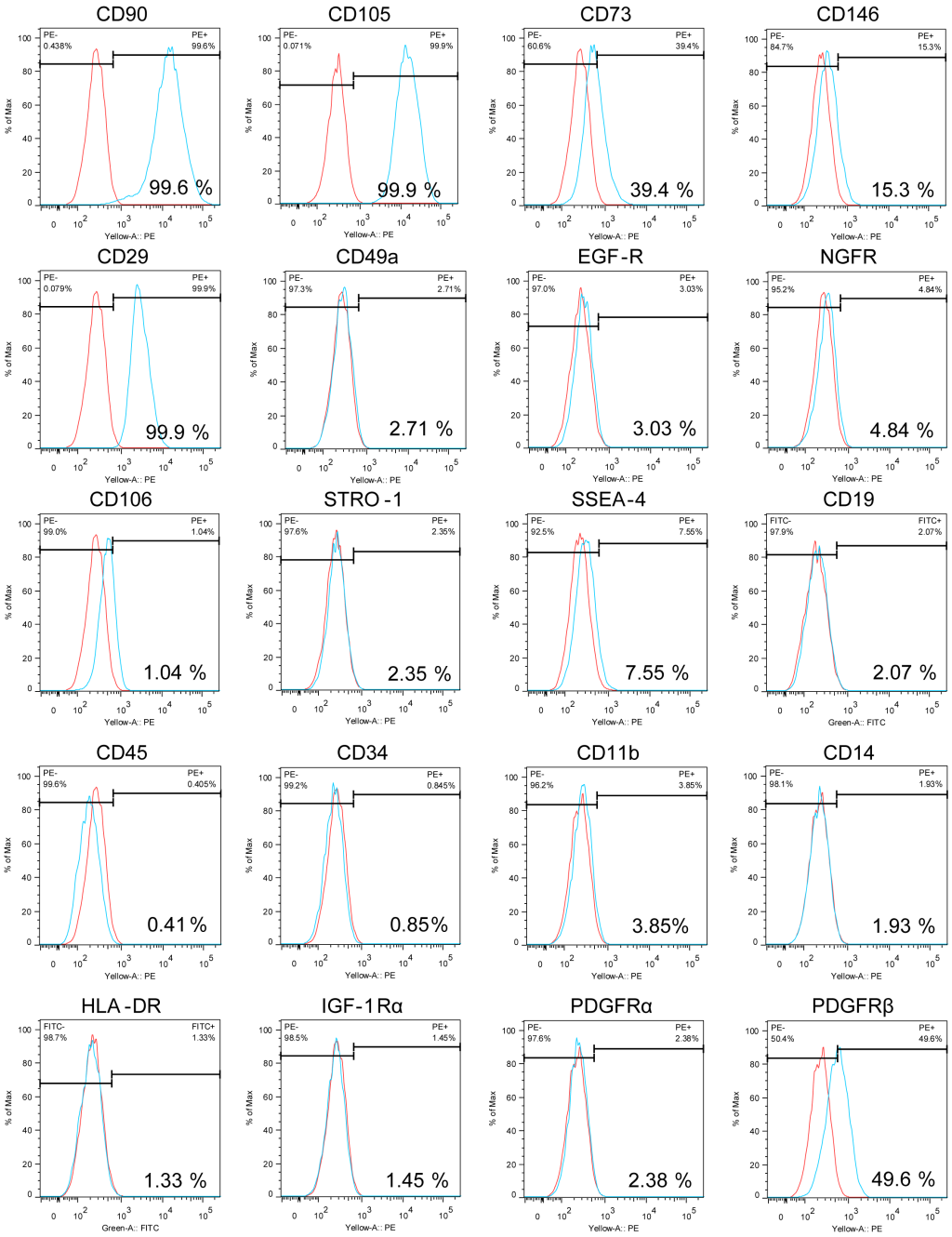

Supplementary Figure 1 – Flow Cytometric Immunophenotyping of hMSCs derived from Donor B. Cells were fixed at passage 6 and analysed by flow cytometry for a range of markers including hMSC markers CD90, CD105 and CD73, hematopoietic markers CD45, CD34, CD11b, CD14 and HLA-DR. Percentage positive cells are marked. The cutoff was set for a false-positive rate of < 2%, based on the relevant isotype control.

A

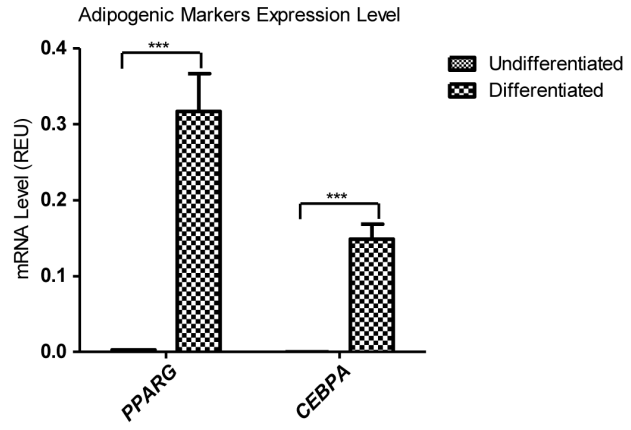

B

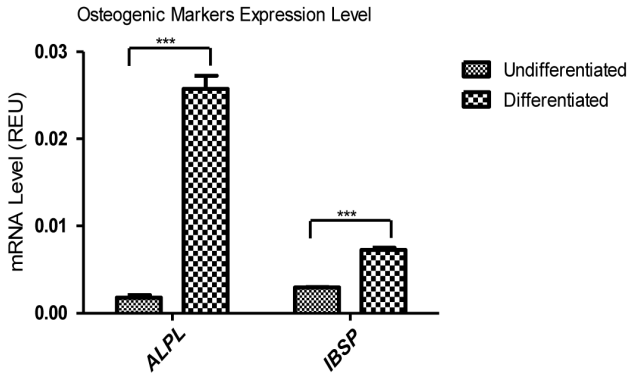

C

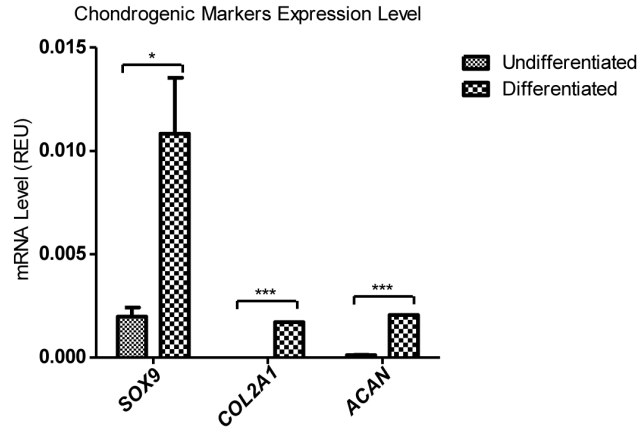

Supplementary Figure 2 – RT-qPCR Quantification of Expression of Multi-lineage Differentiation Markers by hMSCs derived from Donor B. A Adipogenic markers, **B** osteogenic markers, and **C** chondrogenic markers were evaluated from RNA taken from undifferentiated and differentiated cells from Donor B. Columns represent mean mRNA level in relative expression units to reference gene *ACTB*, +/- S.D. of triplicate cultures, * - $p < 0.05$ and *** - $p < 0.001$ by unpaired Student's *t*-test for each gene.

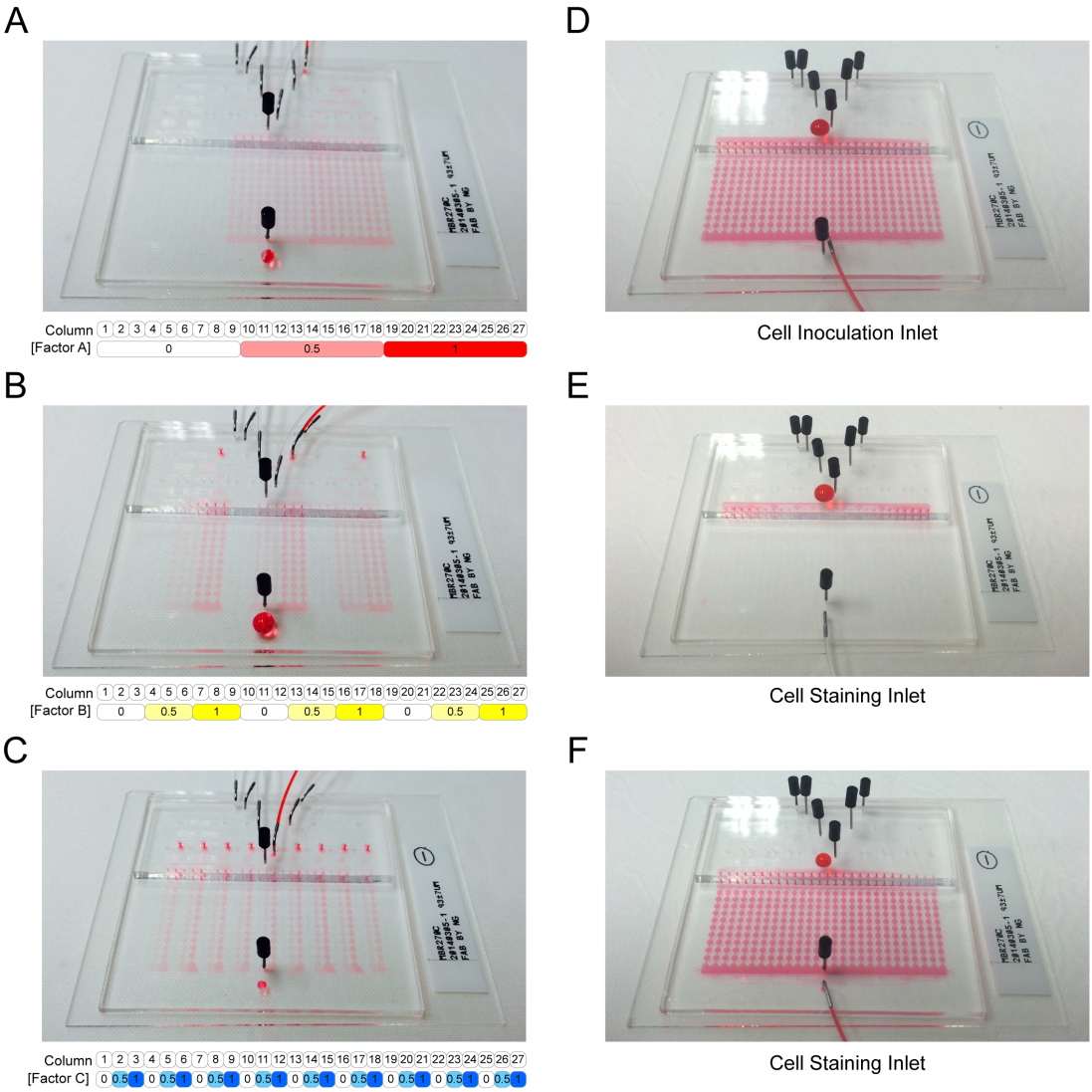

Supplementary Figure 3 - MBA Dye Loading Validation. A-C Photographs of dye loading of Ponceau S solution through individual factor inlets A, B, and C (**A**, **B** and **C**, respectively). The panel below shows the design concentration levels of factor in each column of the array. **D** Dye loading through the cell inoculation inlet, with factor/buffer inlets plugged closed. **E,F** Dye washout (**E**) and re-loading (**F**) from the cell staining inlet, with factor/buffer inlets plugged closed.

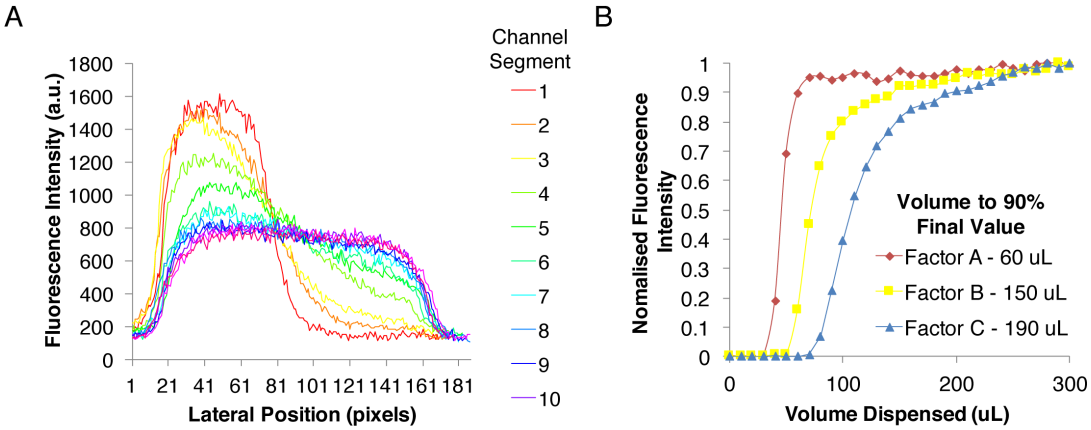

Supplementary Figure 4 – Dynamic Filling and Diffusive Mixing of Alexa Fluor 488-labelled Heparin in the MBA. A Progression of diffusive mixing in the MBA. Pixel intensity profiles were measured across successive microchannel segments during diffusive mixing. Pixel intensity was measured across the channel width in successive segments. **B** Dynamic tracking of establishment of the maximum concentration levels in each of the MBA factor channels A, B and C is shown. Evolution of fluorescence was tracked starting from the beginning of syringe pump flow, for 1 hour at 300 μL/h total flowrate. Volume to 90% final value is shown for each factor channel. All factor channels reached the steady state value within 300 μL volume delivery.

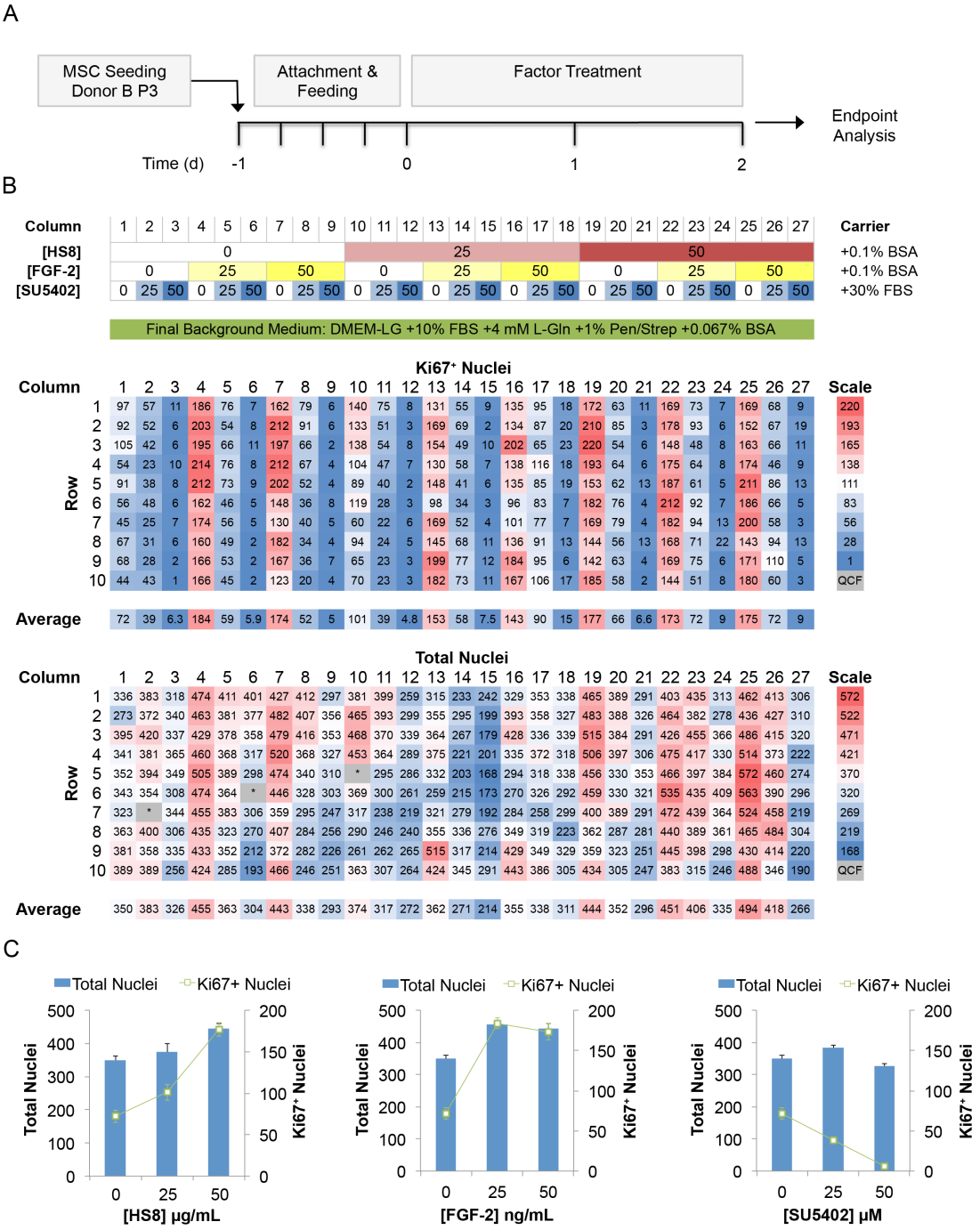

Supplementary Figure 5 - MBA Combinatorial Screening of HS8, FGF-2 and SU5402 in hMSC Donor B. **A** Experimental time course. **B** Top panel: compositions of media in each column of the MBA (HS8, µg/mL; FGF-2, ng/mL; SU5402, µM). Lower panels: Heatmaps of absolute numbers of Ki67+ nuclei, and total nuclei for each chamber in the MBA, corresponding to above compositions. Medium flow was from top (Row 1) to bottom (Row 10) down a column. Mean for each column is given below. QCF: data flagged for quality control issue during image processing. **C** Plots from selected individual MBA columns showing effects of titrations of individual factors (HS8, FGF-2 and SU5402) on total and Ki67+ nuclei. Bars represent mean of all 10 chambers in the relevant column ± SEM.

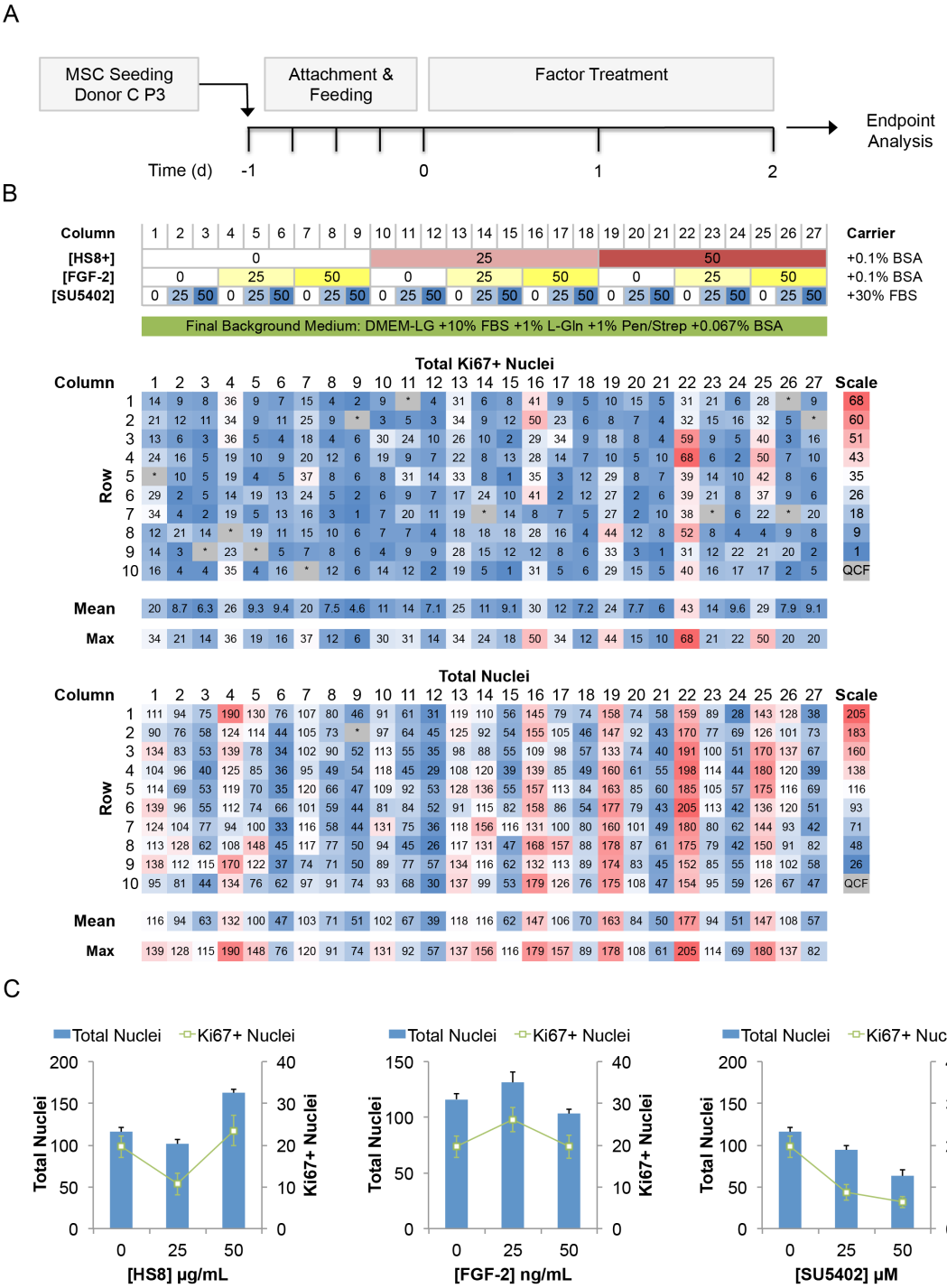

Supplementary Figure 6 - MBA Combinatorial Screening of HS8, FGF-2 and SU5402 in hMSC Donor C. **A** Experimental time course. **B** Top panel: compositions of media in each column of the MBA (HS8, µg/mL; FGF-2, ng/mL; SU5402, µM). Lower panels: Heatmaps of absolute numbers of Ki67⁺ nuclei, and total nuclei for each chamber in the MBA, corresponding to above compositions. Medium flow was from top (Row 1) to bottom (Row 10) down a column. Mean for each column is given below. QCF: data flagged for quality control issue during image processing. **C** Plots from selected individual MBA columns showing effects of titrations of individual factors (HS8, FGF-2 and SU5402) on total and Ki67⁺ nuclei. Bars represent mean of all 10 chambers in the relevant column ± SEM.

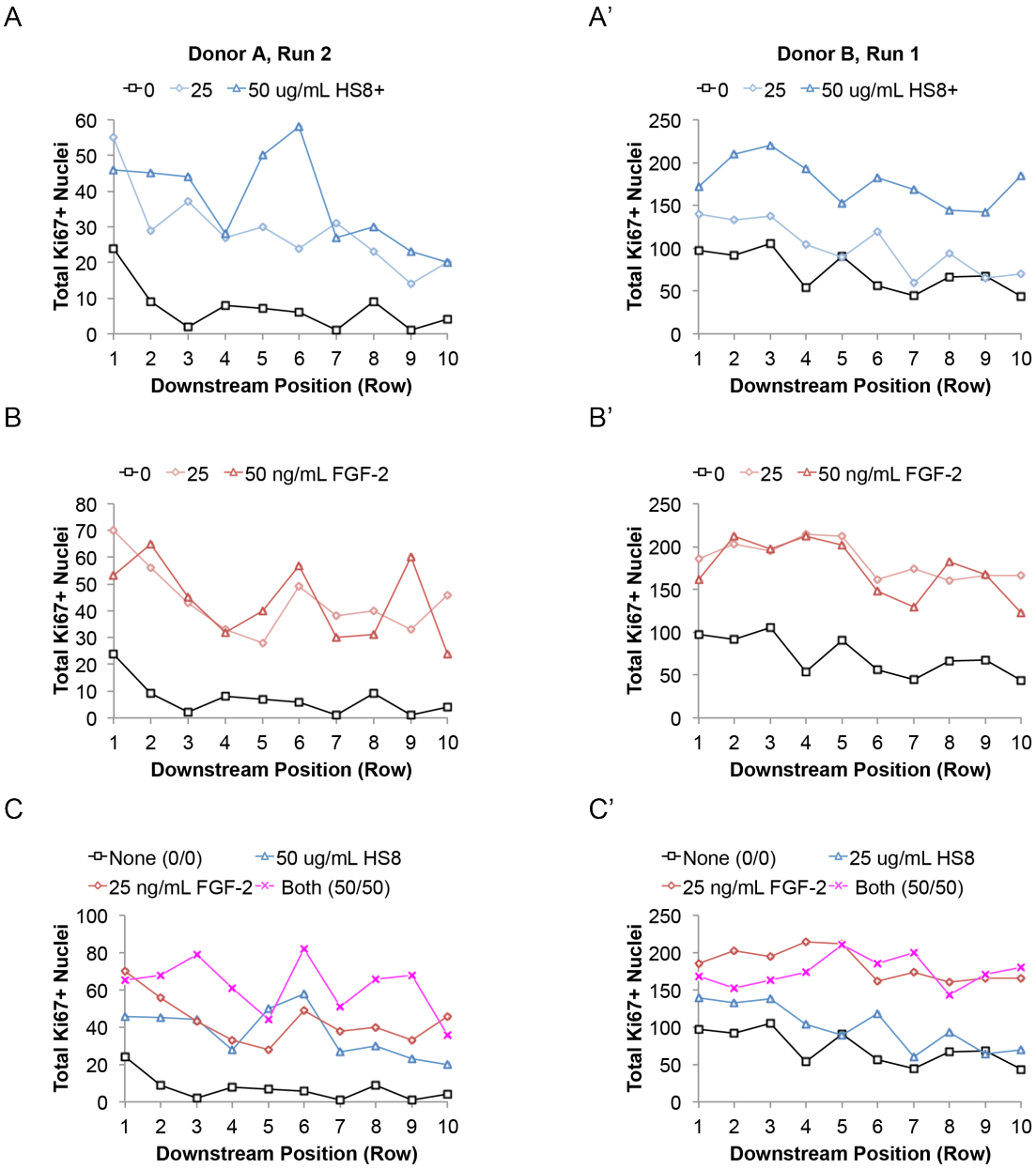

Supplementary Figure 7 – Paracrine profiles of cell responses in replicate runs and donors. A-C Plots for Donor A, Run 2, of Ki67+ nuclei in each chamber versus downstream position (Row coordinate of the chamber) for **A** increasing concentrations of HS8, **B** increasing concentrations of FGF-2, and **C** combinations of HS8 and FGF-2. **A'-C'** Corresponding plots for Donor B, Run 1.

SUPPLEMENTARY TABLES

Supplementary Table 1 – RT-qPCR Probe Information.

Gene Symbol	Gene Name	Assay ID	Reference Sequence
ALPL	alkaline phosphatase, liver/bone/kidney	Hs01029144_m1	NM_000478.4 NM_001127501.2 NM_001177520.1
IBSP	integrin-binding sialoprotein	Hs00173720_m1	NM_004967.3
PPARG	peroxisome proliferator-activated receptor gamma	Hs01115513_m1	NM_005037.5 NM_015869.4 NM_138711.3 NM_138712.3
CEBPA	CCAAT/enhancer binding protein (C/EBP), alpha	Hs00269972_s1	NM_004364.3
SOX9	SRY (sex determining region Y)-box 9	Hs01001343_g1	NM_000346.3
COL2A1	collagen, type II, alpha 1	Hs00264051_m1	NM_001844.4 NM_033150.2
ACAN	aggrecan	Hs00153936_m1	NM_001135.3 NM_013227.3
ACTB	actin, beta	Hs01060665_g1	NM_001101.3